Recent developments in multi-beam echo-sounder processing – The multi-beam potential for sediment classification and water column sound speed estimation

D.G. Simons, A. Amiri-Simkooei, K. Siemes, M. Snellen
TU Delft, Acoustic Remote Sensing group, the Netherlands

Abstract

The multi-beam echo-sounder (MBES) system allows for unprecedented performance in mapping sea- and river-floors with a 100% coverage. It measures with a single acoustic ping the water depths along a wide swathe perpendicular to the ship track using the travel times of the echo signals received in the acoustical beams. MBES ping rates depend on the water depth, but typically are a few tens of Hz. The MBES opening angle is about 150 degrees and contains several hundred narrow beams, thereby providing high-resolution bathymetric maps. The bathymetry is obtained on-line. Frequently, however, knowledge about the water column sound speeds is insufficient for correctly converting the measured travel times to depths. Here, we present a method for estimating the unknown sound speeds from the MBES data itself. This method can be applied as soon as data along overlapping swathes become available. For this semi-online processing, efficient optimization approaches have been implemented. In addition to the travel times, the MBES also provides measurements of the backscatter strengths in each beam, which are known to contain information about the sediment types. We show results of applying a model-based classification method that employs the MBES backscatter data and discriminates between sediments in the most optimal way. The method has been applied for classification of sediments in a large number of areas. Here, we will show classification results for parts of the river Waal and the North Sea.

1. Introduction

The multi-beam echo-sounder (MBES) system allows for unprecedented performance in mapping the bathymetry of sea- and river-floors. The system measures with a single acoustic ping the water depths along a wide swathe perpendicular to the ship track, thereby covering a large area of the sea- or river-floor at once.

The MBES opening angle is about 150 degrees. Beamsteering at reception allows for determining the (two-way) travel-time of the received signals as a function of angle. Water depths along the swathe can be derived from the combination of travel-time and angle, provided that the local sound speed profile in the water column is known (Beaudoin 2004). Typically, the number of beams amounts to several hundreds, thereby providing high resolution bathymetric maps. It is standard practice to carry out MBES surveys with at least a small overlap between adjacent swathes. The sounding density depends on the MBES opening angle, the sailing speed, the overlap and the water depth. For a water depth of 50 m and a ping rate of 5 Hz, typically 1 – 5 soundings per square meter are obtained. The resulting amount of data acquired per day of surveying is at least a few gigabytes. Still, the bathymetry is determined on-line, and the bathymetric map is established on the fly. However, the increased use of the MBES has given rise to additional requests from the user community, resulting in high demands with respect to e.g. the accessibility of the data. Two of these applications are considered in this paper. The focus, however, lies on the physical principles behind these applications.

The first deals with the possibilities to use the MBES in environments with a highly dynamic water column. To capture the resulting variations in the water column sound speeds, a large number of sound speed measurements are needed. Due to the high costs involved, often only a

limited number of measurements are taken. This can result in insufficient knowledge about the sound speeds in the water column, preventing a correct conversion of the measured travel times to depths. The resulting errors in the derived bathymetry may be such that the survey needs to be repeated. An alternative approach is to exploit the redundancy in the MBES measurements, resulting from the overlap between adjacent swathes. The maximum time between measuring two overlapping swathes typically amounts to several hours. Since bottom features, such as mega ripples and sand waves, are not expected to vary significantly on this time-scale, the bottom can be assumed to be stable over the course of the survey. Consequently, the depths as determined from the measured travel times along two overlapping swathes should be the same at equal points on the seafloor. The sound speeds are then estimated by minimizing the difference between the water depths at the overlapping parts of the swathes. This method not only provides the bathymetry for which errors due to insufficient knowledge about the water column sound speeds have been diminished, but it also estimates the water column sound speeds. In principle, the method allows for MBES bathymetric measurements where no sound speed information is acquired as long as the overlap between adjacent swathes is sufficient. This method can be applied as soon as data along overlapping swathes become available. For this semi-online processing, efficient minimization approaches have been implemented.

The second demand from the user community considers the use of acoustic measurements for classifying the sediments. To extract, in addition to bathymetry, also the sediment composition from the MBES measurements would allow for huge cost savings, since it eliminates the need for costly sampling campaigns. Knowledge about the sediment composition is of importance in e.g. marine habitat studies, morphodynamic or sediment transport studies.

It is well-known that the acoustic signals as received by the MBES are affected by the interaction with the sediment. The interaction is dependent on the sediment type. Fine muddy sediments, for example, are known to result in low backscattering, whereas coarse sediments such as gravel result in high backscatter (APL 1994). By employing this knowledge, in theory, the MBES can be used also for sediment classification purposes. However, the process of extracting sediment type from the backscatter measurements requires dedicated processing steps. We have developed a model-based method that employs the MBES backscatter measurements for sediment classification. The method fully accounts for statistical fluctuations in the backscatter intensity and consequently discriminates between sediments in the most optimal way. It estimates both the number of seafloor types present in the survey area and the probability density function for the backscatter strength at a certain angle for each of the seafloor types. Other MBES classification approaches have been developed both by commercial companies and universities. (Simons 2008) (Clarke 1994), (Hellequin 2005) (Canepa 2005) All classification approaches currently can only be applied in a post-processing step and are not yet automated.

Section 2 of this paper describes the approach taken towards eliminating the sound speed induced errors in the bathymetry by estimating the prevailing water column sound speeds. The performance of the method is demonstrated by applying it to MBES data that have been acquired in the Maasgeul, the Netherlands, which is known to be highly variable with regards to the water column sound speed. Section 3 presents the model-based classification method based on the MBES backscatter data. The method has been applied for classification of sediments in a large number of areas. Here, we will present classification results for parts of the river Waal and the North Sea.

2. Compensation of multi-beam echo-sounder (MBES) bathymetric measurements for errors due to the unknown water column sound speed

2.1 Description of the approach

MBES systems emit acoustic pulses in an opening angle of 1 to 2 degrees in along-track direction, and about 150 degrees in the across-track direction. Beamforming in across-track direction is applied to determine the corresponding two-way travel-times for a selected number of arrival angles. Water depths along the swathe, spanned by the across-track opening angle, are determined from the combination of two-way travel-time and angle. Hereto, either propagation along straight sound rays is assumed, or in case the curvature of the sound rays cannot be neglected, ray-trace calculations are carried out.

Inaccurate knowledge about the water column sound speeds results in an erroneous bathymetry in two ways:

1. Errors in the beamsteering process. In case the actual sound speed deviates from the measured sound speed, the actual beamsteering angles differ from the beamsteering angles aimed for, and are unknown.
2. Errors in the conversion from the angle and travel-time combinations to water depths along the swathe.

Figure 1 shows the geometry of a typical MBES survey, consisting of a series of tracks sailed parallel to each other. Track distances are such that a certain overlap exists between adjacent swathes.

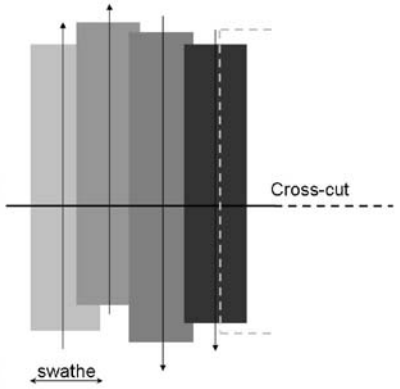

Figure 1. Schematic of an MBES survey. Arrows indicate sailing directions, grey-shaded rectangles the area measured per track.

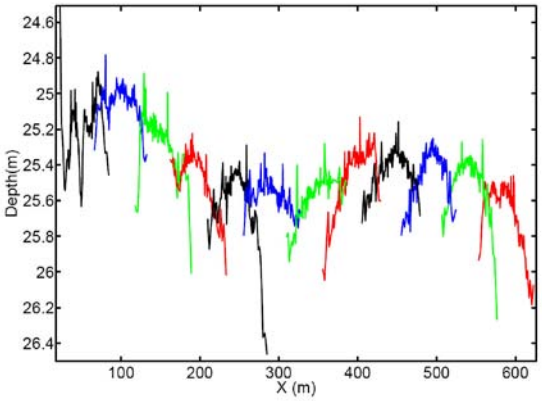

Figure 2. Example of 'droopy' effects along a cross-cut. The MBES measurements were carried out near the entrance to the harbor of Rotterdam.

Figure 2 shows an example of the typical bathymetric behavior along a cross-cut, such as indicated in Figure 1, in case erroneous sound speeds are used. The area in which these MBES were taken is located close to the entrance of the Rotterdam harbor, where mixing of fresh and salt water occurs. The number of parallel tracks amounted to 12. The bathymetry was estimated from the measured travel-times, employing all sound speed information available, i.e., sound speeds measured at the transducer head for the beamsteering and a single sound speed profile for calculating the sound propagation through the water column. The colors indicate the bathymetry as estimated for each of the tracks. Differences in water depths along the overlapping parts of adjacent swathes amount to almost 0.5 m.

Currently, efforts to reduce these effects mainly aim at collecting additional sound speed profile measurements. In addition, research has been carried out to assess the potential of using

oceanographic models for predicting the prevailing sound speeds. (Calder 2004) In this paper, a different approach is taken, where the sound speeds are estimated from the MBES data and no additional sound speed profile measurements are needed.

The method that has been developed for eliminating these effects fully exploits the redundancy of measurements in the overlap region between two adjacent swathes. The measurements are the two-way travel-times per beam and swathe. For estimating the unknown bathymetry and sound speeds, a model is required that predicts these two way travel times, given a set of values for the unknowns. Hereto, the seafloor is modeled with an interpolated grid function, with the water depths at the grid positions being unknowns that need to be determined. We aim to minimize a function that represents the mismatch between measurements and model output, i.e.,

$$E = \sum_{k=1}^{S} \sum_{j=1}^{N} \left(t_{k,j} - T_{k,j} \right)^2 \qquad (1)$$

where N and S are the total numbers of MBES beams and swathes, respectively. The measured two-way travel-times are denoted by $T_{k,j}$. The modeled two-way travel-times are denoted by $t_{k,j}$. The model that calculates $t_{k,j}$, accounts for both the effect of sound speed on the beamsteering and on the propagation through the water column. The unknowns are the sound speed profiles for each of the swathes and the bathymetry. These unknowns should be estimated such that E becomes minimal.

For the minimization we have considered two different optimization techniques:
– The method of Differential Evolution (DE) (Snellen 2008);
– Gauss-Newton (GN).

DE is a global optimization technique and can be seen as a modified version of a Genetic Algorithm. It does not make use of derivatives, but searches within all possible solutions for promising solutions. DE has been applied extensively, showing good to very good performance in locating the global optimum of a function. The advantages lie in its robustness (i.e., its insensitivity to the shape of the energy landscape) and the fact that it does not pose requirements on the behavior of the function considered. The drawback is that it requires a significant number (1000 – 3000) of forward model calculations, in this case model calculations for $t_{k,j}$.

The advantage of GN lies in its efficiency, i.e., it requires much less computations. The drawbacks are that it is a local method, likely to end up in a local minimum in case multiple minima exist, and that it requires expressions for the derivatives of the function with respect to the unknown parameters (unless calculated numerically). These derivatives are dependent on the assumed model for $t_{k,j}$. For the situation at hand, for example, each parameterization of the water column sound speed results in different expressions for $t_{k,j}$.

Based on a series of DE inversions for different parameterizations of a shallow water sound speed profile (constant sound speed, linearly varying sound speed, and a water column consisting of two different layers, each with a different sound speed), all were found to give similar results for the estimated bathymetry. Therefore, for GN we have assumed a constant sound speed throughout the water column. This results in one unknown sound speed for each of the tracks. The unknowns (~250) to be optimized are thus the depths at the grid positions and the sound speeds for each of the swathes.

The optimization procedure is as follows: For the seafloor, we use a fixed grid of closely spaced horizontal positions, denoted X_n in the across-track direction. At every position X_n, Z_n denotes the corresponding water depth. These Z_n are part of the unknowns to be estimated. Between the grid points the depth is interpolated linearly. For every beam j at angle $\theta_{k,j}$, the point where the

acoustic beam impinges on the model seafloor is denoted as ($x_{k,j}$, $z_{k,j}$). Figure 3 shows a schematic overview of this model.

Let the MBES be located at ($X_{k,MBES}$, $Z_{k,MBES}$), then the function for $t_{k,j}$ can be derived by calculating the intersection between the sound ray and the line between the grid points, as illustrated in Figure 3.

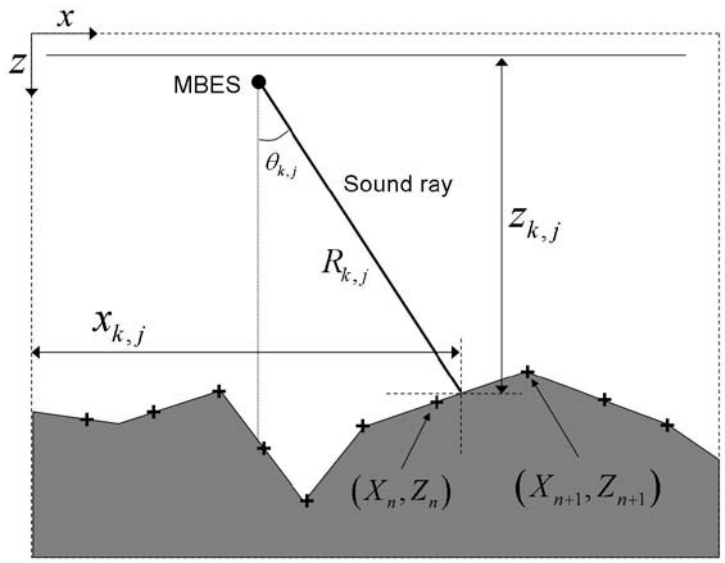

Figure 3. Illustration of the model for $t_{k,j}$. On the right side of the MBES we show the path of a sound ray through water column. The ray impinges at the seafloor in between the grid points X_n and X_{n+1} at coordinates ($x_{k,j}$, $z_{k,j}$). $t_{k,j}$ is calculated as $2R_{k,j}/c$.

The position at which these two lines intersect is given by:

$$x_{k,j} = \frac{\frac{X_{k,MBES}}{\tan\theta_{k,j}} + Z(X_n) - Z_{k,MBES} - X_n \frac{Z(X_{n+1}) - Z(X_n)}{X_{n+1} - X_n}}{\frac{1}{\tan\theta_{k,j}} - \frac{Z(X_{n+1}) - Z(X_n)}{X_{n+1} - X_n}} \tag{2}$$

and

$$z_{k,j} = \frac{x_{k,j} - X_{k,MBES}}{\tan\theta_{k,j}} + Z_{k,MBES} \tag{3}$$

Values for $t_{k,j}$ are calculated employing the water column sound speed c_k as

$$t_{k,j} = \frac{2\left(x_{k,j} - X_{k,MBES}\right)}{c_k \sin\theta_{k,j}} \tag{4}$$

where c_k is the sound speed in swathe k.

For each realization of the unknowns, i.e., the sound speeds c_k and the depths Z_n, values for $t_{k,j}$ are calculated. Minimizing E of Eq. (1) implies a search for those values of the unknowns that minimize the difference between the measured ($T_{k,j}$) and calculated travel times ($t_{k,j}$). To solve for Eq. (1) in a least-squares sense requires the iterative Gauss-Newton approach. For this, the expressions for the derivatives of $t_{k,j}$ to all unknowns have been determined. In general, two to three iterations were found to be sufficient for localizing the optimal values for Z_n and c_k. Either

the optimized depths can be used directly as the corrected bathymetry, or the optimized sound speeds can be used to recalculate the bathymetry for each beam and each ping.

In (Snellen, 2009) simulations are presented to assess the required overlap. It was found that both an increasing noise level and a decreasing overlap result in increased deviations of the estimations from the true bathymetry and sound speeds, but that still the deviation is limited, with mean errors in the sound speed and bathymetry seldom exceeding 1 m/s and 0.2 m.

2.2 Results

The method has been applied to MBES data that were collected in the Maasgeul, the Netherlands. The black rectangle in Figure 4 indicates the area of the measurements. The data have been collected during a standard survey, during which a single sound speed profile was measured. The sound speed values at the MBES transducer were measured continuously.

The left plot of Figure 5 shows the bathymetry as determined from the MBES measurements, where all available sound speed information was used for converting the measured travel times to water depths. Artifacts running parallel to the sailing direction are clearly visible. These show a typical 'droopy' structure, indicating that they are caused by errors in the conversion from travel times to water depths due to insufficient knowledge about the prevailing sound speed profiles. These droopy effects are most pronounced in the outer beams. However, the bathymetric errors are also present directly underneath the sonar.

The plot on the right of Figure 5 shows the bathymetry as obtained after application of the refraction-correction method described above. Clearly the artifacts have been eliminated. The beam trawl marks (depths of several dm's) are still visible.

It can be concluded that the proposed method strongly increases the potential of the MBES to accurately measure the bathymetry in environments with a strongly varying water column. The availability of efficient optimization techniques allows for application of the bathymetry correction in real time, i.e., as soon as the first overlaps become available.

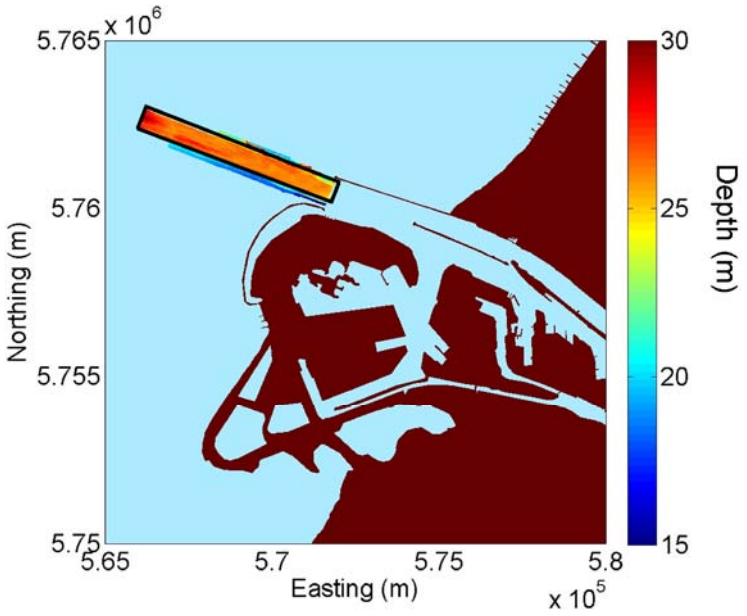

Figure 4. The Maasgeul area (close to the Rotterdam harbor) where the MBES measurements were taken.

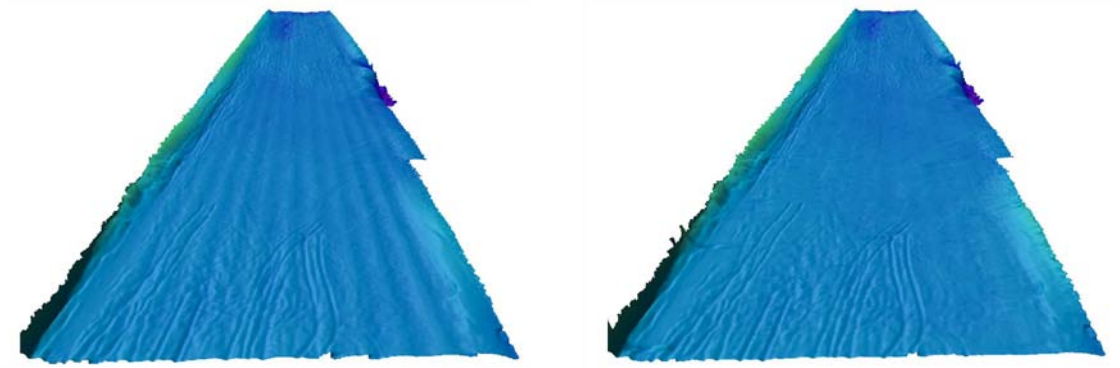

Figure 5. Left plot: Bathymetry as determined from the MBES measurements before application of the proposed method. Right plot: bathymetry obtained from application of the correction method.

3. Sediment classification with the multi-beam echo-sounder

3.1 Description of the method

The approach presented classifies the sediments in an area based on the measured backscatter. The backscatter intensity varies with incidence angle. This angular dependence masks effects of variation in sediment type and morphology in the backscatter images. Therefore, MBES systems apply corrections to the measured backscatter intensities to eliminate this angle dependence, e.g. by assuming Lambert's law. The backscatter images obtained from the MBES after angle correction are comparable to those obtained with a side-scan sonar system (SSS). These maps can be used for classification purposes by resolving textures or spatial variability in the data., e.g. as in (Blondel 2009). On the other hand, the variation of the backscatter strength versus angle with sediment type can potentially be used for classification (Simons 2008), (Clarke 1994) (Canepa 2005). A problem in this latter approach arises for areas where the sediment type varies along the swathe. In this case, it is difficult to discriminate between the angular variation itself and real sediment type variation along the swathe.

Therefore, we have selected an alternative approach. The approach proposed here employs the backscatter data still containing the angular dependence. It is, therefore, not dependent on the corrections applied to eliminate this angular dependence. However, instead of using the angular behavior of the backscatter strength as the classifying parameter, it uses backscatter measurements per angle. Additionally, it accounts for the ping-to-ping variability of the backscatter intensity that partly masks the information about sediment characteristics. The classification method employs the backscatter values (in dB) per receiver beam, i.e., backscatter values that have been obtained from averaging (or filtering) over the N_s independent scatter pixels in a receiver beam. Corrections for propagation losses and footprint are applied, and backscatter values are provided for each of the MBES beams.

Due to the small pulse length T_p employed by the shallow water MBES systems (typically ~100 μs) the signal footprint is also small. The beam footprint is determined by the water depth H, the beam angle and the MBES transducer characteristics, and typically is much larger than the signal footprint. The number of scatter pixels N_s per beam footprint for a beam at angle θ with the vertical is given by

$$N_s(\theta) = \frac{\frac{H\Omega_{rx}}{\cos^2\theta}}{\frac{cT_p}{2\sin\theta}} \qquad (5)$$

with c the water column sound speed and Ω_{rx} the beam opening angle in the across-track direction. This expression only holds for beams away from normal incidence.

If N_s is sufficiently large for the central limit theorem to hold, the backscatter values per beam are distributed according to a normal distribution. For water depths of a few meters, as encountered e.g. in river environments, N_s is not sufficiently large for the assumption of a normal distribution to hold, and the measured backscatter strengths are averaged over a number of subsequent pings and beams to increase N_s (Amiri-Simkooei 2009).

Based on the assumption of normally distributed backscatter strengths per sediment type, we apply the following approach towards classification of the sediments.

Step 1: Nonlinear curve fitting. The algorithm starts by fitting a model to the histogram of measured backscatter strengths. The data consist of all averaged backscatter data as measured for a certain angle (or set of angles in shallow water situations). The model that we fit to the histograms, therefore, consists of a sum of m Gaussian probability density functions (PDFs), each PDF representing a sediment type with mean backscatter strength $\overline{y}_k$ and standard deviation σ_{yk} (both in dB), i.e.,

$$f(y_j \mid x) = \sum_{k=1}^{m} c_k \exp\left(-\frac{(y_j - \overline{y}_k)^2}{2\sigma_{yk}^2} \right) \tag{6}$$

with $f(y_j \mid x)$ the value of the model at backscatter value y_j, and vector x containing the unknown parameters, i.e., $x = (\overline{y}_1, \ldots, \overline{y}_m, \sigma_{y_1}, \ldots, \sigma_{y_m}, c_1, \ldots, c_m)^T$. As a measure for the match between model and measurements we consider the χ^2 value

$$\chi^2 = \sum_{j=1}^{M} \frac{\left(n_j - f(y_j \mid x) \right)^2}{\sigma_j^2} \tag{7}$$

with M the number of bins in the histogram and n_j the number of y_j occurrences. Assuming that the n_j are Poisson distributed, the variances σ_j^2 are equal to n_j. The unknown parameters are determined by minimizing Eq. (7).

Parameter m, i.e., the number of detectable sediment types present, is estimated by carrying out the fitting procedure for an increasing number of m, until further increasing m, no longer results in an improvement of the goodness of the fit. Figure 6 presents an illustration of this procedure. The thick solid black line in the figures corresponds to the histogram of the measures backscatter strengths. The fit is represented by the red line, with the individual PDFs represented by the thin black lines (4, 5, 6, and 7 for the different subplots, respectively). The goodness-of-fit criterion is defined as the reduced χ^2 – value $\chi_\nu^2 = \chi^2 / \nu$ being close to one, where $\nu = M - 3m$ are the degrees of freedom.

Step 2: Acoustic classes identification. After step 1, both the PDFs for each of the sediment types and the number of sediment types are known. We assume all hypotheses to be equally likely. Then, by applying the Bayes decision rule for multiple (m) hypotheses H_i, a sediment type is assigned to each measurement as follows:

$$\text{accept } H_k \text{ if } \quad \underbrace{\max}_{H_i} f(y_j \mid H_i) = f(y_j \mid H_k) \quad \text{with } i = 1, \ldots, m \tag{9}$$

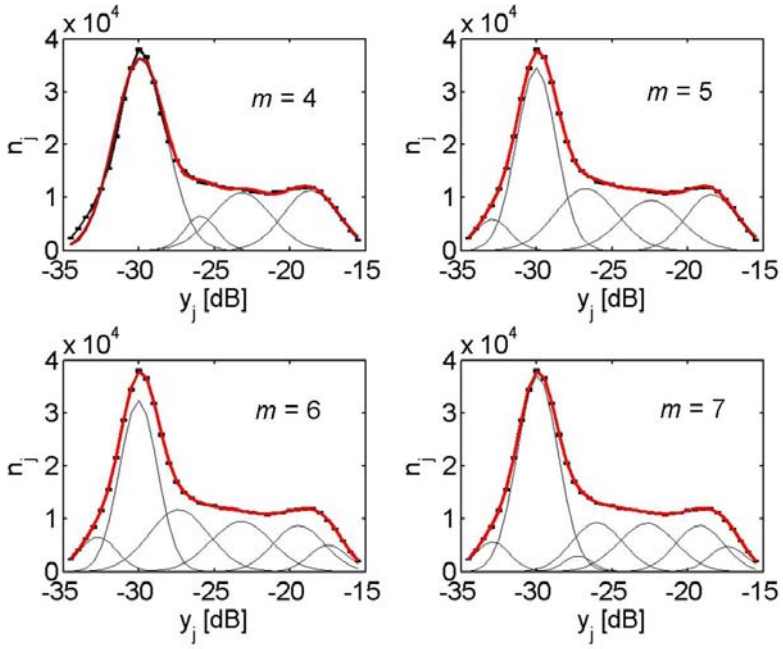

Figure 6. Histograms of measured backscatter data (60 degree beam) fitted to the model for m = 4, 5, 6 and 7, respectively.

This means that we choose the hypothesis that, given the observation *y*, maximizes the likelihood $f(y \mid H)$. We, therefore, have to determine the intersections of the *m* normal PDFs, resulting from the fitting procedure of Step 1. This results in *m* non-overlapping acceptance regions A_k.

Step 3: Assigning sediment type to acoustic classes. Now, a sediment type needs to be assigned to each of the acceptance regions. The result of this step can be accomplished by a comparison of the $\bar{y}_k$ values with a combination of data found in the literature, model outcomes and knowledge of the surveyed area based on e.g. cores or samples.

Step 4: Quality assessment. Based on the so-called decision matrix of the multiple-hypothesis-testing problem, probabilities of incorrect decision are determined.

Step 5: Mapping. By plotting sediment type versus position, e.g. with different colors representing different sediment types, a classification map of the area is obtained.

3.2 Results

The approach described in section 3.1 has been applied to MBES data acquired in a large number of different areas, with different sediment types. For the current paper, we present results for two different areas.

The first area is the Cleaver Bank area in the North Sea, the Netherlands. The upper plot of Figure 7 shows the bathymetry in the area, indicating water depths from ~30 to ~60 m. The data were acquired in 2004. The MBES used for the measurements was an EM3000 dual-head system, working at a frequency of 300 kHz. The pulse length amounts to 150 μs. The opening angles in both the along-track and across-track direction amounts to 1.5°. In total 254 beams are formed by the system. In practice, however, the number of beams at which measurements are taken is less and typically amounts to 160.

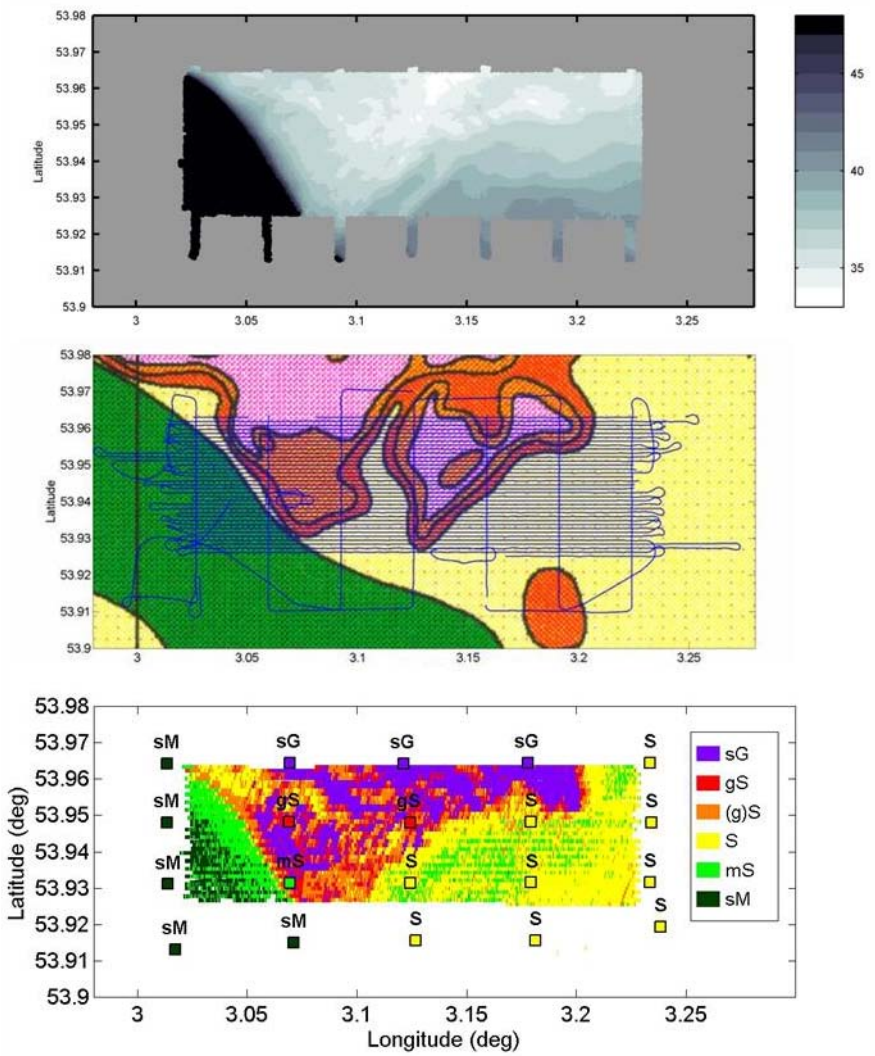

Figure 7. Upper plot) The bathymetry in the Cleaver Bank area. Middle plot) The tracks sailed during the survey, superimposed on a geological map of the area. Lower plot) Classification of the sediments by application of the proposed classification method. Also indicated is the Folk class as a function of position as determined from the grabs. The sediment types present are, i.e., sandy gravel (sG), gravelly sand (gS), slightly gravely sand ((g)S), sand (S), muddy sand (mS), and sandy mud (sM).

The data were provided as raw data files (4.5 GB) from which the backscatter strength as a function of angle and position has been extracted. The middle plot of Figure 7 shows the tracks sailed during the survey. The ping rate is about 5 Hz. The survey lasted for about 32 hours, resulting in ~600.000 pings collected during the survey. For the water depths in the area which range from 30 to 60 m, this corresponds to a 1 – 5 measurements per square meter.

For each ping the backscatter strength at a predefined angle is selected. By applying the method as described in the previous section it is found that, based on the backscatter strengths, 6 sediment types could be discerned in the surveyed area. Samples of the sediment were employed to assign a sediment type to each of the acoustic classes. The resulting classification map is shown at the bottom of Figure 7. Also shown in this plot are the sediment types according to the samples. Clearly, the acoustic classification method reveals a distribution of the sediments over the area that is in good agreement with the distribution indicated by analysis of the sediment samples.

Figure 8 shows the classification map for the second MBES data set, acquired along a part of the river Waal, close to St. Andries. Again the system is a 300 kHz MBES with a maximum of 254 beams. The ping rate is about 35-40 Hz, resulting in ~2 million pings in the surveyed area. Sediments in this area are coarser then those at the Cleaver Bank. As with the Cleaver Bank area, the acoustic classification results are in very good agreement with the sediment samples.

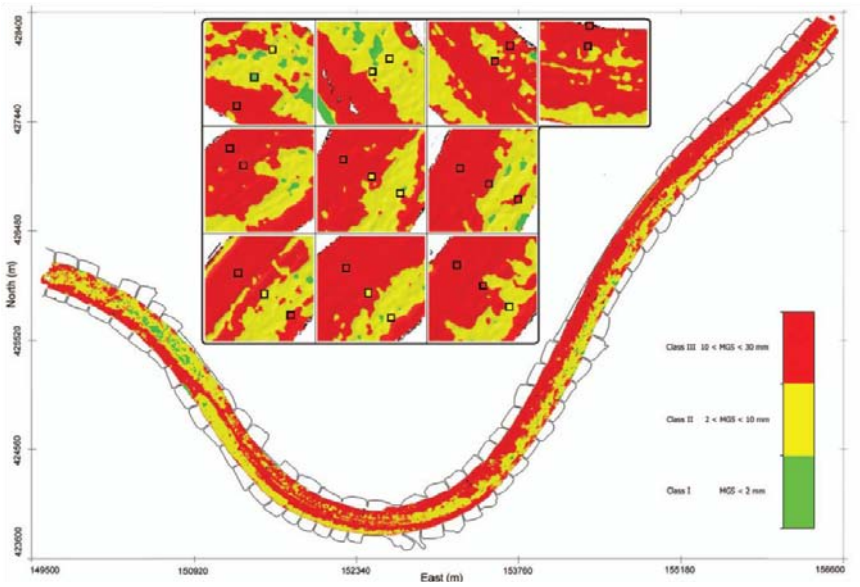

Figure 8. Acoustic classification map for an area of the Waal, close to St. Andries. The three colors indicate the three acoustic classes. The results of the sample analysis are shown by the squares. MGS indicates the mean grain sizes.

4. Summary and conclusions

In this paper two methods are described that focus on improving the performance of MBES systems. For both, efficient access to the individual data points within the large number of measurements is essential.

The first aims at eliminating errors in the bathymetry due to erroneous sound speed information by employing the overlap between adjacent MBES swathes. In principle, this method allows for MBES surveys where no information regarding the prevailing sound speeds is acquired. The approach has been optimized with regards to computational efficiency. Consequently, the method can be employed in real-time during the survey. The only requirement is that there exists overlap between adjacent swathes.

In addition, the performance of the MBES with regards to classification of the sediments is demonstrated. For the research presented in the paper, the classification has been carried out after the survey. However, for practical situations where it might be of interest to establish a picture of the sediment distribution while surveying, another approach can be selected, where each new measurement is added to the previous measurements. The fitting procedure has then to be repeated during the survey, thereby building up and refining the overview of the sediment distribution in the area of the survey.

The combination of high-resolution bathymetry and high-resolution classification results can provide important new insights in the mechanisms governing the sediment distribution. Further future developments in this field will be to fully exploit the entire time series, i.e. the complete received signal per beam, for improved classification. This requires storing the received signal

for each ping and each beam, whereas currently the signal is reduced to two parameters, being the two-way travel time and backscatter strength. The advantage of obtaining more information is, therefore, counteracted by a significant increase in data rate with at least a factor of 100 to 1000. Allowing classification approaches that employ the complete signal per beam to be applied real-time is expected to require a significant research effort.

Acknowledgements

We would like to thank Ben Dierikx, Simon Bicknese, and the Dutch Directorate-General for Public Works and Water Management for fruitful discussions and valuable MBES data sets. Also we would like to thank the Dutch Hydrographic Service for providing us with MBES data. This work is financially supported by the Dutch Directorate-General for Public Works and Water Management, the Netherlands Geodetic Commission, and the Technical University of Delft.

References

APL-UW High-frequency Ocean Environmental Acoustic Models Handbook, Technical Report, APL-UW TR 9407, AEAS 9501, October 1994.

Amiri-Simkooei, A.R., Snellen, M., Simons, D.G., 'Riverbed sediment classification using MBES backscatter data', Journal of the Acoustical Society of America 126, 2009, p. 1724-1738.

Beaudoin, J., Hughes Clarke, J.E. and Bartlett, J.E., 'Application of surface sound speed measurements in postprocessing for multi-sector multibeam echosounders', International Hydrographic Review 5, 2004, p. 26-31.

Blondel, Ph., and Gómez Sichi, O., 'Textural analyses of multibeam sonar imagery from Stanton Banks, Northern Ireland continental shelf', Applied Acoustics 70, 2009, p. 1288–1297.

Calder, B., Kraft, B., de Moustier, C., Lewis, J., and P. Stein, 'Model-based refraction correction in intermediate depth multibeam echosounder survey', In Proceedings of the Seventh European Conference on Underwater Acoustics, Delft, the Netherlands, 2004, p. 795-800.

Clarke, J.H., 'Toward remote seafloor classification using the angular response of acoustic backscattering: a case study from multiple overlapping GLORIA data', IEEE J Ocean Eng 19, 1994, p. 112-26.

Hellequin, L., Boucher, J., Lurton, X., 'Processing of high-frequency multibeam echo sounder data for seafloor characterization', IEEE J Ocean Eng 28, 2005, p. 78–89.

Canepa, G., and Pouliquen, E., 'Inversion of geo-acoustic properties from high frequency multibeam data', in Proceedings of boundary influences in high frequency shallow water acoustics, Bath, UK, 2005, p. 233-40.

Simons, D.G. and Snellen, M., 'A comparison between modeled and measured high frequency bottom backscattering', in Proceedings of the European Conference on Underwater Acoustics, Paris, France, 2008, p. 639-644.

Snellen, M., and Simons, D.G., 'An assessment of the performance of global optimisation methods for geo-acoustic inversion', Journal of Computational Acoustics 16, 2008, p.199-223.

Snellen M., Siemes K., Simons, D.G., 'An efficient method for reducing the sound speed induced errors in multi beam echo sounder bathymetric measurements', in Proceedings of the Underwater Acoustic Measurements Conference, Nafplion, Greece, 2009, p. 1155-1162.